

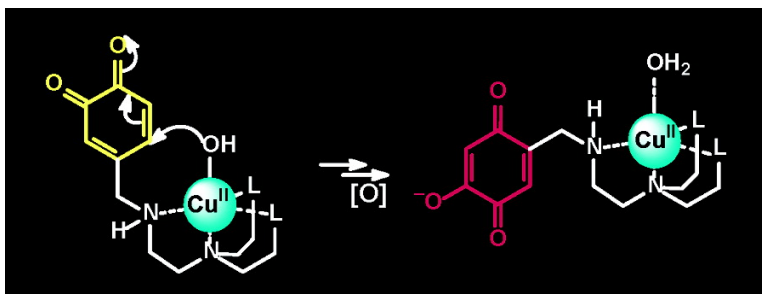
Article

A Dopaquinone Model That Mimics the Water Addition Step of Cofactor Biogenesis in Copper Amine Oxidases

Ke-Qing Ling, and Lawrence M. Sayre

J. Am. Chem. Soc., **2005**, 127 (13), 4777-4784 • DOI: 10.1021/ja0455603 • Publication Date (Web): 11 March 2005

Downloaded from <http://pubs.acs.org> on March 25, 2009



More About This Article

Additional resources and features associated with this article are available within the HTML version:

- Supporting Information
- Links to the 2 articles that cite this article, as of the time of this article download
- Access to high resolution figures
- Links to articles and content related to this article
- Copyright permission to reproduce figures and/or text from this article

[View the Full Text HTML](#)

A Dopaquinone Model That Mimics the Water Addition Step of Cofactor Biogenesis in Copper Amine Oxidases

Ke-Qing Ling and Lawrence M. Sayre*

Contribution from the Department of Chemistry, Case Western Reserve University,
Cleveland, Ohio 44106

Received July 23, 2004; E-mail: lms3@case.edu

Abstract: The consensus mechanism for biogenesis of the 2,4,5-trihydroxyphenylalanine quinone (TPQ) cofactor in copper amine oxidases involves a key water addition to the dopaquinone intermediate. Although hydration of *o*-quinones seems straightforward and was implicated previously in aqueous autoxidation of catechols to give ultimately hydroxyquinones, a recent study (Mandal, S.; Lee, Y.; Purdy, M. M.; Sayre, L. M. *J. Am. Chem. Soc.* **2000**, *122*, 3574–3584) showed that the observed hydroxyquinones arise not from hydration, but from addition to the *o*-quinones of H₂O₂ generated during autoxidation of the catechols. In the enzyme case, hydration of dopaquinone is proposed to be mediated by the active site Cu(II). To establish precedent for this mechanism, we engineered a catechol tethered to a Cu(II)-coordinating unit, such that the corresponding *o*-quinone could be generated in situ by oxidation with periodate (to avoid generation of H₂O₂). Thus, coordination of 4-((2-bis(2-pyridylmethyl)amino)ethylamino)methyl)-1,2-benzenediol (**1**) to Cu(II) and subsequent addition of periodate resulted in rapid formation of the TPQ-like corresponding hydroxyquinone. Hydroxyquinone formation was seen also using Zn(II) and Ni(II), but not in the absence of M(II). Under the same conditions, periodate oxidation of the simple catechol 4-*tert*-butylcatechol does not give hydroxyquinone in the presence or absence of Cu(II). M^{II}OH₂ pK_a data for the Cu(II), Zn(II), and Ni(II) complexes with the pendant tetradentate ligand in the masked (dimethyl ether) catechol form, and kinetic pH–rate profiles of the metal-dependent hydroxyquinone formation from periodate oxidation of catechol **1**, suggested a rate-limiting addition step of the ligand-coordinated M^{II}OH to the *o*-quinone intermediate. This study represents the first chemical demonstration of a true *o*-quinone hydration, which occurs in cofactor biogenesis in copper amine oxidases.

Introduction

Copper amine oxidases (CAOs) are a ubiquitous family of copper-containing enzymes found in bacteria, yeast, plants, and mammals.¹ In microorganisms, CAOs permit the use of low molecular weight amines as sources of carbon and nitrogen, whereas in plants, CAOs are involved in developmental processes and wound healing.^{2,3} In mammals, CAOs play important roles in a variety of physiological processes including detoxification, signaling, cell growth and maturation, cell adhesion, lipid trafficking, drug binding, and glucose homeostasis, and are also implicated in a number of human pathological conditions such as diabetes, atherosclerosis, cardiovascular diseases, and Alzheimer's disease.⁴ Most CAOs utilize an active

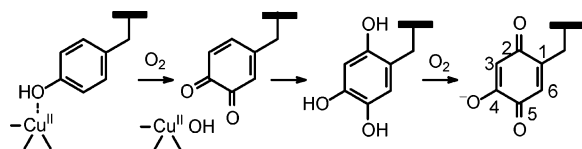
site tyrosine-derived 2,4,5-trihydroxyphenylalanine quinone (TPQ) cofactor to catalyze oxidative deamination of primary amines to aldehydes and ammonia at the expense of reducing oxygen to hydrogen peroxide.^{1,5}

TPQ cofactor biogenesis was studied extensively in the 1990s using both wild-type and active site mutant apoproteins of different sources, showing it to be a posttranslational self-processing reaction.⁶ Early biogenesis proposals^{6e–h,7} suggested an initial monooxygenation of phenol to give catechol, which subsequently was oxidized to an *o*-quinone intermediate. However, more recent proposals suggested a direct 4e[−] oxidation

- (1) (a) Knowles, P. F.; Dooley, D. M. In *Metal Ions in Biological Systems*; Sigel, H., Sigel, A., Eds.; Marcel Dekker: New York, 1994; Vol. 30, pp 361–403. (b) Klinman, J. P. *Chem. Rev.* **1996**, *96*, 2541–2561.
- (2) McIntire, W. S.; Hartman, C. In *Principles and Applications of Quinoproteins*; Davidson, V. L., Ed.; Marcel Dekker: New York, 1993; pp 97–171.
- (3) (a) Rea, G.; Laurenzi, M.; Tranquilli, E.; D'Ovidio, R.; Federico, R.; Angelini, R. *FEBS Lett.* **1998**, *437*, 177–182. (b) Walters, D. R. *Phytochemistry* **2003**, *64*, 97–107.
- (4) For recent reviews, see: (a) Yu, P. H.; Wright, S.; Fan, E. H.; Lun, Z. R.; Gubisne-Harberle, D. *Biochim. Biophys. Acta* **2003**, *1647*, 193–199. (b) Boomsma, F.; Bhaggoo, U. M.; van der Houwen, A. M.; van den Meiracker, A. H. *Biochim. Biophys. Acta* **2003**, *1647*, 48–54. (c) O'Sullivan, J.; Unzeta, M.; Healy, J.; O'Sullivan, M. I.; Davey, G.; Tipton, K. F. *Neurotoxicology* **2004**, *25*, 303–315. (d) Matyus, P.; Dajka-Halasz, B.; Foldi, A.; Haider, N.; Barlocco, D.; Magyar, K. *Curr. Med. Chem.* **2004**, *11*, 1285–1298.

- (5) (a) Janes, S. M.; Mu, D.; Wemmer, D.; Smith, A. J.; Kaur, S.; Maltby, D.; Burlingame, A. L.; Klinman, J. P. *Science* **1990**, *248*, 981–987. (b) Brown, D. E.; McGuirl, M. A.; Dooley, D. M.; Jane, S. M.; Mu, D.; Klinman, J. P. *J. Biol. Chem.* **1991**, *266*, 4049–4051. (c) Duine, J. A. *Eur. J. Biochem.* **1991**, *200*, 271–284. (d) Mure, M.; Mills, S. A.; Klinman, J. P. *Biochemistry* **2002**, *41*, 9269–9278. (e) Mure, M. *Acc. Chem. Res.* **2004**, *37*, 131–139.
- (6) (a) Cai, D.; Klinman, J. P. *J. Biol. Chem.* **1994**, *269*, 32039–32042. (b) Matsuzaki, R.; Fukui, T.; Sato, H.; Ozaki, Y.; Tanizawa, K. *FEBS Lett.* **1994**, *351*, 360–364. (c) Choi, Y.-H.; Matsuzaki, R.; Fukui, Y.; Shimizu, E.; Yorifuji, T.; Sato, H.; Ozaki, Y.; Tanizawa, K. *J. Biol. Chem.* **1995**, *270*, 4712–4720. (d) Hanlon, S. P.; Carpenter, K.; Hassan, A.; Cooper, R. A. *Biochem. J.* **1995**, *306*, 627–630. (e) Matsuzaki, R.; Suzuki, S.; Yamaguchi, K.; Fukui, Y.; Tanizawa, K. *Biochemistry* **1995**, *34*, 4524–4530. (f) Tanizawa, K. *J. Biochem.* **1995**, *118*, 671–678. (g) Klinman, J. P. *J. Biol. Chem.* **1996**, *271*, 27189–27192. (h) Nakamura, N.; Matsuzaki, R.; Choi, Y.-H.; Tanizawa, K.; Sanders-Loehr, J. *J. Biol. Chem.* **1996**, *271*, 4718–4724.
- (7) Rinaldi, A. C.; Rescigno, A.; Rinaldi, A.; Sanjust, E. *Bioorg. Chem.* **1999**, *27*, 253–288.

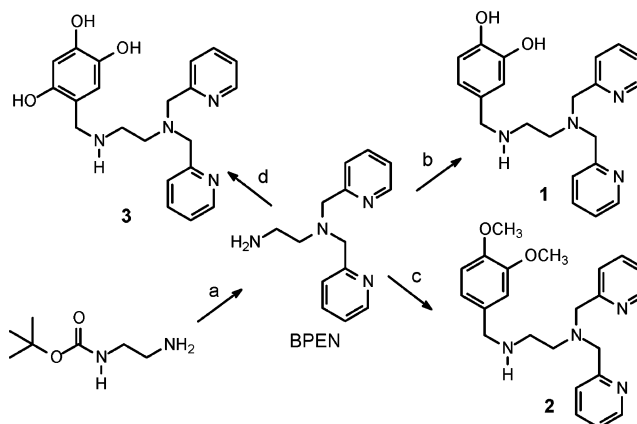
Scheme 1



of the phenol to give *o*-quinone.⁸ The current consensus mechanism for the overall $6e^-$ oxidation biogenesis⁹ involves interaction of the tyrosine phenol with the nearby trihistidinyl- Cu^{II} ,¹⁰ resulting in O_2 -dependent monooxygenation to generate the dopaquinone (DPQ) intermediate and a residual trihistidinyl- $\text{Cu}^{\text{II}}\text{OH}$, followed by conjugate addition of the Cu^{II} -bound water to form the reduced triol form of TPQ,⁸ which then undergoes autoxidation to TPQ (Scheme 1). However, since the water delivered to C2 of the mature cofactor was shown to derive from bulk solvent and not O_2 ,^{6h} the initially O_2 -derived Cu^{II} -bound water would have to exchange with bulk solvent water before conjugate addition to the *o*-quinone took place. Ligand exchange on Cu^{II} is known to be rapid.

The chemically most challenging step in the proposed biogenesis mechanism is the first Cu^{II} -mediated monooxygenation, since most copper-mediated oxygenation reactions in biology entail a Cu^{I} -mediated activation of O_2 . In contrast, the step involving conjugate addition of water to the *o*-quinone seems straightforward, and was implicated earlier in the aqueous autoxidation of dopamine to form the neurotoxin 6-hydroxydopamine¹¹ as well as in model TPQ cofactor biogenesis systems that start with the catechol as a predecessor to the *o*-quinone.¹² However, we recently demonstrated that starting directly with *o*-quinones, water addition is very slow, even at elevated pH, and that TPQ-like hydroxyquinones formed in the aqueous autoxidation of catechols arise from conjugate addition to *o*-quinone of H_2O_2 generated in the catechol autoxidation step.¹³ We therefore suggested that the *o*-quinone hydration step in TPQ biogenesis must be a facilitated event, possibly by the active site Cu^{II} .¹³ Although the latest TPQ biogenesis proposals typically depict the *o*-quinone being hydrated by the trihistidinyl- $\text{Cu}^{\text{II}}\text{OH}$ species (which has evidently undergone exchange),^{8,9} there is so far no direct chemical precedent for such a facilitated *o*-quinone hydration.

In this paper, using a H_2O_2 -free protocol, we have further confirmed that hydration of a simple DPQ model quinone does

Scheme 2^a

^a Reagents and conditions: (a) (1) 2-picoyl chloride hydrochloride/ $\text{NaOH}/\text{THF}/\text{H}_2\text{O}/50^\circ\text{C}$; (2) HCl/EtOH ; (b) (1) 3,4-dihydroxybenzaldehyde/ $\text{HOAc}/\text{MeOH}/\text{NaBH}_4$; (2) $\text{Boc}_2\text{O}/\text{TEA}/\text{DCM}$; (3) HCl/EtOH ; (c) (1) 3,4-dimethoxybenzaldehyde/ $\text{HOAc}/\text{MeOH}/\text{NaBH}_4$; (2) $\text{Boc}_2\text{O}/\text{TEA}/\text{DCM}$; (3) HCl/EtOH ; (d) (1) 2,4,5-trihydroxybenzaldehyde/ $\text{HOAc}/\text{MeOH}/\text{NaBH}_4$; (2) $\text{Boc}_2\text{O}/\text{TEA}/\text{DCM}$; (3) HCl/EtOH .

not occur at physiological pH. We then have developed a novel DPQ model with a pendant Cu^{II} -chelating complex that readily accomplishes Cu^{II} -mediated quinone hydration at neutral pH. To our knowledge, this is the first chemical demonstration of a true *o*-quinone hydration, proposed in the consensus mechanism of TPQ biogenesis.

Results and Discussion

Synthesis of Models. The target model in its catechol version (**1**) was synthesized by reductive amination of 3,4-dihydroxybenzaldehyde with *N,N*-bis(2-pyridylmethyl)ethylenediamine (BPEN) (Scheme 2). Direct isolation of **1** is inconvenient due to its zwitterionic property, and pure product was obtained by Boc protection and then deprotection of the purified tri-Boc-protected ligand **1** under mild conditions (HCl/EtOH). To study the Cu^{II} coordination chemistry and to characterize the final hydroxyquinone product, the redox-inactive dimethylcatechol **2** and the triol **3** were also synthesized by similar reductive aminations with BPEN of 3,4-dimethoxybenzaldehyde and 2,4,5-trihydroxybenzaldehyde, respectively, using the same Boc protection–deprotection approach. All three were obtained as the corresponding tri-HCl salts.

Acid–Base Properties and Coordination Chemistry of Model Ligand **2 with Selected Metal Ions.** Ligand **2** forms a 1:1 complex with Cu^{II} as shown by UV–vis titration of Cu^{II} with the free base form of **2** (see the Experimental Section and Figure S1 in the Supporting Information). The acid–base properties of **2** and its coordination chemistry with Cu^{II} , Zn^{II} , and Ni^{II} were studied by potentiometric pH titration (Figure 1A).¹⁴ The multistep protonation constants $\text{p}K_1$, $\text{p}K_2$, and $\text{p}K_3$ of ligand **2** were found to be 9.07, 5.00, and 3.08, respectively. The fourth protonation occurs at strongly acidic pH. This explains why ligand **2** was obtained as a tri- rather than tetra-HCl salt. The stability constants ($\log K_f$) for formation of the 1:1 complexes between **2** and Cu^{II} , Zn^{II} , and Ni^{II} were all > 10 (Table 1). Of particular interest are the acid dissociation $\text{p}K_a$ values for the metal-bound water in the 1:1 com-

- (8) (a) Ruggiero, C. E.; Smith, J. A.; Tanizawa, K.; Dooley, D. M. *Biochemistry* **1997**, *36*, 1953–1959. (b) Wilce, M. C. J.; Dooley, D. M.; Freeman, H. C.; Guss, J. M.; Matsunami, H.; McIntire, W. S.; Ruggiero, C. E.; Tanizawa, K.; Yamaguchi, H. *Biochemistry* **1997**, *36*, 16116–16133. (c) Ruggiero, C. E.; Dooley, D. M. *Biochemistry* **1999**, *38*, 2892–2898. (d) Dooley, D. M. *J. Biol. Inorg. Chem.* **1999**, *4*, 1–11.
- (9) Brazeau, B. J.; Johnson, B. J.; Wilmot, C. M. *Arch. Biochem. Biophys.* **2004**, *428*, 22–31.
- (10) (a) Chen, Z.-W.; Schwartz, B.; Williams, N. K.; Li, R.; Klinman, J. P.; Mathews, F. S. *Biochemistry* **2000**, *39*, 9709–9717. (b) Dove, J. E.; Schwartz, B.; Williams, N. K.; Klinman, J. P. *Biochemistry* **2000**, *39*, 3690–3698. (c) Schwartz, B.; Dove, J. E.; Klinman, J. P. *Biochemistry* **2000**, *39*, 3699–3707. (d) Schwartz, B.; Olgin, A. K.; Klinman, J. P. *Biochemistry* **2001**, *40*, 2954–2963. (e) Kim, M.; Okajima, T.; Kishishita, S.; Yoshimura, M.; Kawamori, A.; Tanizawa, K.; Yamaguchi, H. *Nat. Struct. Biol.* **2002**, *9*, 591–596.
- (11) (a) Garcia-Moreno, M.; Rodriguez-Lopez, J. N.; Martinez-Ortiz, F.; Tudela, J.; Varon, R.; Garcia-Canovas, F. *Arch. Biochem. Biophys.* **1991**, *288*, 427–434. (b) Rodriguez-Lopez, J. N.; Varon, R.; Garcia-Canovas, F. *Int. J. Biochem.* **1993**, *1175*–1182. (c) Senoh, S.; Creveling, C. R.; Udenfriend, S.; Witkop, B. *J. Am. Chem. Soc.* **1959**, *81*, 6236–6240.
- (12) Rinaldi, A. C.; Porcu, M. C.; Curreli, N.; Rescigno, A.; Finazziagro, A.; Pedersen, J. Z.; Rinaldi, A.; Sanjust, E. *Biochem. Biophys. Res. Commun.* **1995**, *214*, 559–567.
- (13) Mandal, S.; Lee, Y.; Purdy, M. M.; Sayre, L. M. *J. Am. Chem. Soc.* **2000**, *122*, 3574–3584.

- (14) Martell, A. E.; Motekaitis, R. J. *Determination and Use of Stability Constants*, 2nd ed.; VCH: New York, 1992.

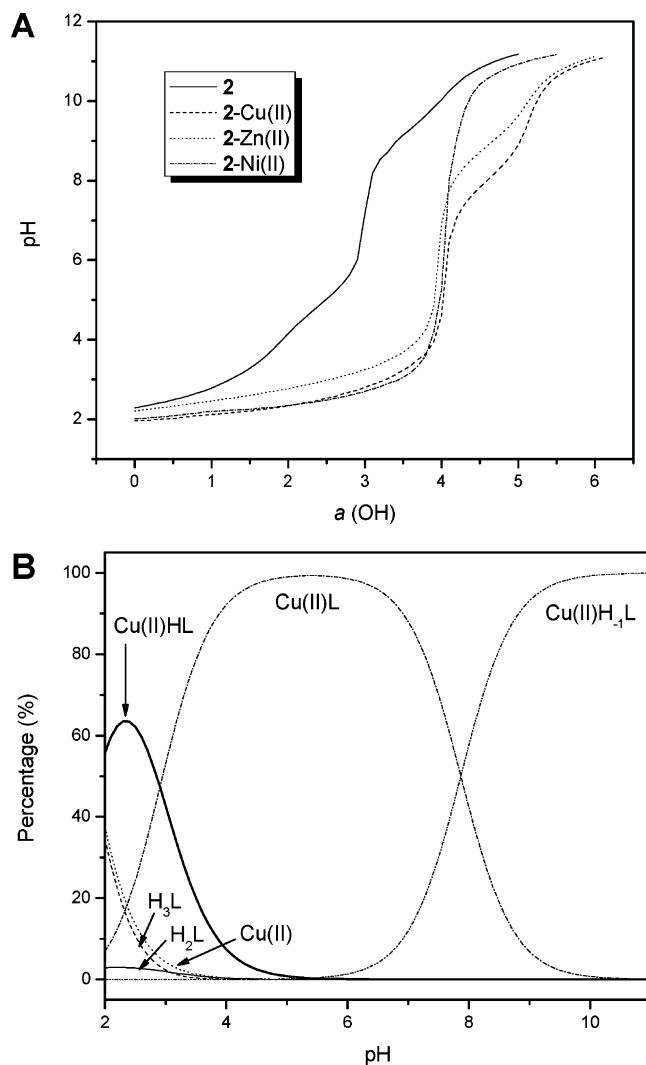


Figure 1. (A) Titration curves of 5.00 mM **2**·3HCl or a mixture of 5.00 mM **2**·3HCl and 5.00 mM M(II) with NaOH in 0.15 M KNO₃ aqueous solution in the presence of 5.00 mM HNO₃. (B) Speciation diagram for 5.00 mM **2**/5.00 mM Cu(II) in 0.15 M KNO₃ as a function of pH at 25 °C.

Table 1. Equilibrium Constants of 1:1 Complexes of **2** with Selected Metal Ions^a

	Cu(II)	Zn(II)	Ni(II)
log K_f	13.2	11.1	13.0
pK _a of LM ^{II} OH ₂	7.87	8.60	10.6

^a Calculated from potentiometric pH titration data in 0.15 M aqueous KNO₃ at 25 °C.

plexes, which show a rank order consistent with the Lewis acidity of these divalent metal ions. The speciation diagrams¹⁴ for **2**-M(II) as a function of pH show domination of two consecutive acid–base equilibria, M^{II}HL/M^{II}L and M^{II}L/M^{II}H₂L in acidic and neutral–basic regions, respectively, as exemplified by **2**-Cu(II) (Figure 1B). The involvement of these metal species was further confirmed by UV–vis monitoring of the potentiometric pH titration of **2**-Cu(II), and the λ_{\max} values of these species were 672 nm for Cu^{II}HL, 844 nm for Cu^{II}L, and 837 nm for Cu^{II}H₂L (Figure S2 in the Supporting Information).

Periodate Oxidation of 4-tert-Butylcatechol Does Not Give Hydroxyquinone in pH 7.5 Buffer. To study quinone hydration, we have chosen to generate the required but only metastable *o*-quinone species in situ by periodate oxidation of cate-

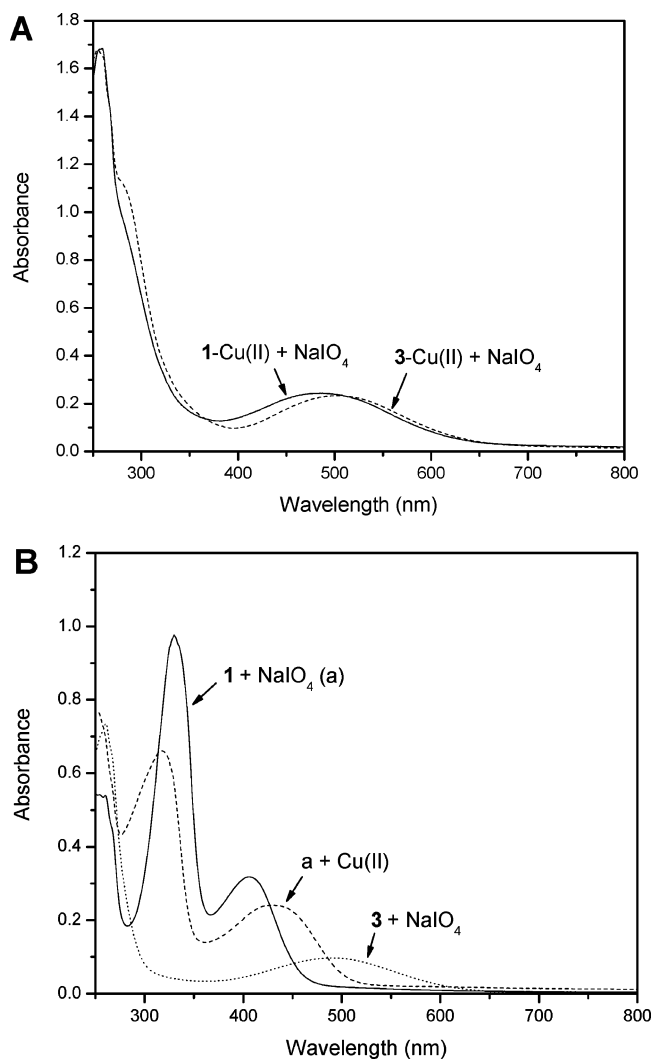
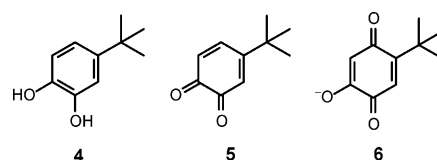


Figure 2. Periodate oxidation of **1** or **3** in 0.05 M pH 7.5 MOPSO buffer at 25 °C: (A) UV–vis spectra recorded immediately upon mixing of a solution of **1**-Cu(II) or **3**-Cu(II) (1 × 10⁻⁴ M) with NaIO₄ (2 × 10⁻⁴ M); (B) UV–vis spectra recorded immediately upon mixing of a solution of **1** or **3** (5 × 10⁻⁵ M) with NaIO₄ (1 × 10⁻⁴ M), and then, in the case of **1**, recorded again upon addition of Cu(II) (5 × 10⁻⁵ M). In all cases, no further spectral changes were observed after the first spectrum was recorded.

chols. Also, to avoid complications arising from production of H₂O₂ via autoxidation events, an excess of periodate was maintained, ensuring immediate oxidation of not only the triol generated in the hydration reaction, but also any catechol arising from reduction of *o*-quinone by *o*-quinone decomposition products.¹³ Formation of hydroxyquinone under such conditions can thus be taken as a reliable indicator of “true” quinone hydration.

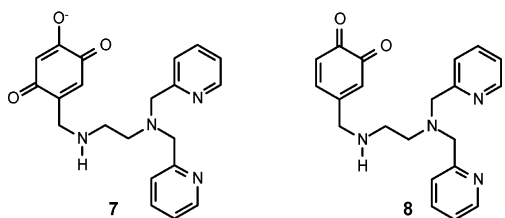
To validate the periodate protocol, we reevaluated the behavior of 4-*tert*-butyl-1,2-benzoquinone (**5**) generated in situ by periodate oxidation of catechol **4**, which, under autoxidation conditions, affords hydroxyquinone **6**.¹³



Incubation of **4** with 2 mol equiv of NaIO₄ in 0.05 M pH 7.5 β -hydroxy-4-morpholinepropanesulfonic acid (MOPSO) buffer

instantaneously generated quinone **5** ($\lambda_{\max} = 400 \text{ nm}$),¹³ which then converted ($t_{1/2}$ of $\sim 1 \text{ h}$) in an isosbestic fashion to a new species with $\lambda_{\max} \approx 250 \text{ nm}$, without apparent formation of any hydroxyquinone **6**, as shown by time-dependent difference UV–vis spectroscopy (Figure S3 in the Supporting Information). Identical behavior was seen starting with authentic **5** under the same conditions (data not shown). Bleaching of authentic **6** was found to be fairly slow under the same conditions (3% over 1 h), and did not generate the 250 nm species (Figure S3), suggesting that quinone hydration is not occurring under this condition. The presence of 1 equiv of CuSO_4 (free or coordinated 1:1 to bis(2-pyridylethyl)amine) in this system was found to alter the stability of various intermediates and products, but we saw no evidence for even transient generation of **6** (Supporting Information). Thus, in an intermolecular sense, Cu(II) appears unable to sufficiently promote *o*-quinone hydration in this simple model.

Behavior of the Catechol Ligand **1 in pH 7.5 Buffer.** In contrast to the unsuccessful hydration of quinone **5**, when the catechol ligand model **1** was first coordinated with 1 equiv of Cu(II), and then subjected to periodate oxidation in 0.05 M pH 7.5 MOPSO buffer, the solution immediately turned red ($\lambda_{\max} = 500 \text{ nm}$), the expected color of the TPQ-like hydroxyquinone anion **7**–Cu(II). Formation of **7** was verified by spectral comparison with authentic **7**–Cu(II) generated from periodate oxidation of **3**–Cu(II) under the same conditions (Figure 2A), and further confirmed by HPLC analysis after reduction to authentic triol **3** (see the Experimental Section and Figure S6 in the Supporting Information). The yield of **7**–Cu(II) was almost quantitative (93% by UV–vis), and the reaction was so fast that the *o*-quinone intermediate **8**–Cu(II) could not be detected by routine spectrophotometry.



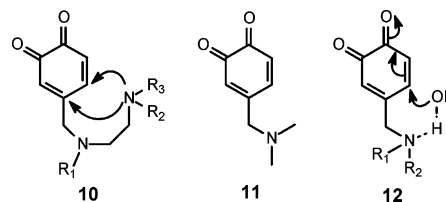
Under the same conditions, complexes **1**–Zn(II) and **1**–Ni(II) also underwent quinone hydration to give **7**–Zn(II) (UV–vis yield 92%) and **7**–Ni(II) (UV–vis yield 82%), but the red color was seen to form more slowly, with a transient yellow color, presumably representing the intermediate *o*-quinone, being seen in the case of Ni(II). In contrast, reaction of **1**–Co(II) was complicated by rapid deterioration of the hydroxyquinone product as verified by periodate oxidation of **3**–Co(II) under the same conditions. The $\sim 500 \text{ nm}$ absorbance observed for all M(II) complexes of **7** suggests that the hydroxyquinone anion is not coordinated to the metal center in the product complex, even though the enolate O2 should be capable of doing so geometrically. Such coordination would be expected to induce a significant blue shift of the hydroxyquinone chromophore due to charge localization,¹⁵ as implicated by the fact that inactive forms of copper amine oxidases, whose

(15) In fact, we have observed an 81 nm blue shift of the hydroxyquinone chromophore (from 493 to 412 nm) in another synthetic hydroxyquinone ligand model upon coordination with Cu(II).¹⁶

crystal structures show coordination of the TPQ enolate O4 to Cu(II), are colorless.^{5e}

Importantly, periodate oxidation of **1** in the absence of M(II) instantaneously afforded a light yellow solution ($\lambda_{\max} = 330$ and 407 nm) with no evidence for the copresence of even a trace of hydroxyquinone **7** (compare to the spectrum for periodate oxidation of **3** under the same conditions, Figure 2B). In addition, subsequent addition of 1 equiv of Cu(II) (or Zn(II) or Ni(II)) did not stimulate generation of **7** (Figures 2B and S7 in the Supporting Information). These results show that hydration of the *o*-quinone moiety of **8** can only be achieved when it is generated at the point M(II) is prebound to the ligand system, and that, in the absence of M(II), the transiently formed **8** rapidly converts to a species with λ_{\max} at 330 and 407 nm.

The fate of quinone **8** in the absence of metal ion is unclear, as all attempts to determine the nature of the product(s) have failed so far due to continuous decomposition of the product mixture during isolation. In fact, a whole series of variously *N*-substituted quinone models **10**, generated by periodate oxidation of the corresponding catechols in pH 7.5 MOPSO buffer, all decompose very quickly in the absence of M(II) and show a UV–vis spectral behavior ($\lambda_{\max} \approx 330$ and 405 nm) very similar to that of “decomposed” **8**.¹⁶ On this basis and the finding that quinone model **11** is much more stable than **8** under the same conditions,¹⁶ we conclude that the rapid decomposition of **8** and its relatives (**10**) is most likely initiated by an *intramolecular conjugate addition* of the distal tertiary amino group to the quinone ring, which apparently is more favorable than the *intermolecular* water addition. We have observed intramolecular conjugate addition reactions for other *o*-quinones containing pendant OH, COOH, and NH_2 nucleophiles.¹⁶



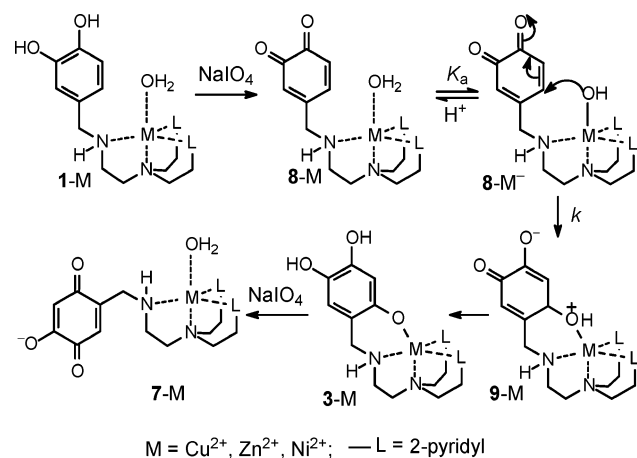
Interestingly, the M(II)-mediated quinone hydration was found to be significantly inhibited by phosphate buffer; e.g., periodate oxidation of **1**–Cu(II) in 0.05 M pH 7.5 phosphate buffer gave **7**–Cu(II) in only 48% yield (by UV–vis), along with a major side product that is identical with that formed when 1 equiv of Cu(II) is added to a preoxidized mixture of **1** in the same buffer (Figure S8 in the Supporting Information).

The crystal structures of Cu(II) complexes with tripodal tetradentate ligands are well-known,¹⁷ and the Cu(II) may adopt geometries ranging from typical trigonal bipyramidal to distorted square pyramidal depending on the nature of the ligands used. Because the UV–vis spectrum of complex **2**–Cu(II) in aqueous solution exhibits a λ_{\max} at 844 nm rather than 650 nm, we conclude that Cu(II) mainly adopts a trigonal bipyramidal rather than a distorted square pyramidal geometry,^{17b} with the tertiary amine and a fifth water ligand occupying the two axial positions. We believe that this axial water molecule plays a key role in

(16) Ling, K. Q.; Sayre, L. M. Unpublished results.

(17) (a) Nagao, H.; Komeda, N.; Mukaida, M.; Suzuki, M.; Tanaka, K. *Inorg. Chem.* **1996**, *35*, 6809–6815. (b) Weitzer, M.; Schatz, M.; Hampel, F.; Heinemann, F. W.; Schindler, S. *J. Chem. Soc., Dalton Trans.* **2002**, 686–694.

Scheme 3



the observed quinone hydration (Scheme 3). The inhibition of quinone hydration by phosphate can be interpreted in terms of preferential coordination of phosphate (substituting for the water) as the fifth metal ligand. We see no reason for phosphate to inhibit the quinone hydration reaction if it were not for the strict metal ion dependence of this process.

It should be noted that *o*-quinones such as **11** should serve as reasonable models to mimic water addition through a general-base catalysis (GBC) mechanism (a favorable six-membered ring transition state is depicted in **12**). The fact that none of them display significant conversion to the corresponding hydroxyquinone¹⁶ suggests that the GBC mechanism is not a facile process in solution compared to other possible decomposition pathways of these highly unstable *o*-quinones.

Kinetics of M(II)-Mediated Quinone Hydration. In contrast to the very rapid Cu(II)-mediated quinone hydration at neutral pH, at lower pH (e.g., pH 4 acetate buffer), the intermediacy of the *o*-quinone **8**-Cu(II) in formation of the final product **7**-Cu(II) can be seen by routine spectrophotometry (Figure 3). A clean isosbestic conversion of **8**-Cu(II) ($\lambda_{\max} = 380$ nm) to **7**-Cu(II) is observed. A reasonable mechanism for formation

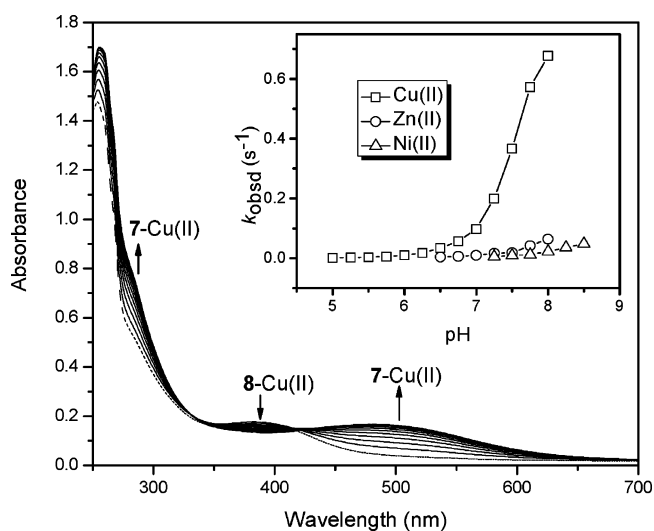


Figure 3. Time-dependent (40 s interval) hydroxyquinone formation from **1**-Cu(II) (1×10^{-4} M) in 0.05 M pH 4.00 acetate buffer upon periodate (2×10^{-4} M) oxidation at 25 °C. Inset: pH–rate profiles of hydroxyquinone formation from **1**-Cu(II), **1**-Zn(II), and **1**-Ni(II) upon periodate oxidation in mixed universal buffer (0.1 M acetate, 0.05 M MES, and 0.05 M HEPES) at 10 °C.

of hydroxyquinone **7** is shown in Scheme 3. Control experiments demonstrated that oxidations of catechol and triol by periodate were essentially instantaneous, even at 5 °C. Thus, the rate-limiting step for formation of **7** in Figure 3 must correspond to a reaction other than periodate oxidation of catechol or triol intermediates. Since aromatization of unstable tautomer **9** to triol **3** should also be very fast, we believe that the rate-limiting step is quinone hydration after equilibrium deprotonation of the Cu(II)-bound water (Scheme 3). According to this mechanism, the pH–rate profiles should reflect the critical ionization equilibrium.

To obtain kinetic data over a wide pH range, which is not a function of the particular buffer used in each corresponding pH range,¹⁸ we introduced a mixed “universal” buffer solution composed of 0.1 M acetate, 0.05 M MES, and 0.05 M HEPES. The pH–rate profiles for formation of **7**-M(II) from the **1**-Cu(II), **1**-Zn(II), and **1**-Ni(II) complexes in this universal buffer are shown in Figure 3 (inset). Rate data could not be obtained at high pH (>8.5 for Ni(II), >8.0 for Zn(II) and Cu(II)) either because of rapid decomposition of complexes **7**-M(II) or apparent complexities in the solubility behavior of the metal complexes (especially Cu(II)) at basic pH.¹⁹ In the pH range shown, the pH–rate profiles for all three M(II) complexes show a monotonic increase with increasing pH that is consistent with a rate-limiting quinone hydration step associated with an ionization equilibrium. A least-squares fit of the Cu(II) data to $k_{\text{obsd}} = kK_{\text{app}}/(\alpha_{\text{H}^+} + K_{\text{app}})$ yielded a first-order rate constant k of 1.28 ± 0.15 s⁻¹, and an apparent ionization constant $\text{p}K_{\text{app}}$ of 7.93 ± 0.09 , which is close to the titrated $\text{p}K_{\text{a}}$ of **2**-Cu(II) (Table 1). Though there are insufficient data to derive kinetic constants in the cases of Zn(II) and Ni(II), the pH–rate profiles are consistent with kinetic $\text{p}K_{\text{app}}$ values that match the titrated $\text{p}K_{\text{a}}$ values for **2**-M(II).

For the enzyme, the rate of quinone hydration in TPQ biogenesis is unknown because it is not the rate-limiting step. The half-life of the overall biogenesis process for AGAO has been reported to be about 30 s.^{8c} Assuming that the hydration step is about 10 times this fast, it would be comparable to the half-life of Cu(II)-mediated hydration in our model system, which can be estimated to be a few seconds at pH 7.

Conclusion. We have obtained a model (**1**) that allows access to a DPQ-like intermediate (**8**), which simulates the Cu(II)-mediated *o*-quinone hydration step proposed in the consensus mechanism of TPQ biogenesis.^{8–10} The success of this model compared to simpler models (e.g., **5**) where *o*-quinone decomposition predominates over hydration appears to reflect the favorable *intramolecular* delivery of the Cu(II)-bound OH, a better nucleophile than bulk solvent water, to the *o*-quinone C2. Thus, the occurrence of DPQ hydration in the enzyme must reflect in part the entropic advantage afforded by the active site orienting the DPQ intermediate with respect to the trihistidinyl-Cu^{II}OH to facilitate the desired water addition.⁸ The active site

(18) As an example, the observed rate constant (0.345 s⁻¹) for formation of **7**-Cu(II) from periodate oxidation of **1**-Cu(II) in 0.05 M pH 5.5 MES buffer is nearly 10-fold faster than that (0.0404 s⁻¹) of the same reaction in 0.05 M pH 5.5 acetate buffer at 25 °C, showing a significant inhibitory effect of acetate on the quinone hydration due to ligand exchange.

(19) Above pH 8.0, the rate for the Cu(II) complex decreased sharply in a non-bell-shaped manner. Although there was no obvious precipitation, it seems that the intermediate **8**-Cu(II)OH may be self-associating in a way that is equivalent to insolubilization. Interestingly, in the presence of the organic cosolvent dioxane (slower rates), the rate was seen to increase monotonically all the way up to pH 8.5.

could possibly also ensure the success of the hydration step by suppressing decomposition pathways.

It is curious that following delivery of the Cu^{II}OH to C2 and subsequent oxidation, the Cu(II) in our model does not coordinate to the newly delivered oxygen (a partial oxyanion). The same scenario holds for the case of the active enzyme, presumably due to a spatial reorientation of the TPQ ring. While we do not suggest that our model simulates the proposed cofactor reorientation, the affinity of the Cu(II) for the C2 oxyanion is apparently not so high (it is a delocalized rather than localized oxyanion), and this factor should contribute to the lack of coordination observed both in the model and in the active enzyme.

A recent quantum mechanical study on TPQ biogenesis suggested that the active site Cu^{II}OH species might be acting as a general-base catalyst to mediate DPQ hydration rather than as the attacking nucleophile.²⁰ A GBC mechanism would obviate the issue of water exchange strictly required if the Cu(II)-bound OH generated in the initial monooxygenation reaction is indeed the attacking nucleophile. While we have not carried out studies to exclude the operation of GBC in our model, direct nucleophilic attack takes advantage of a six-membered ring transition state, and the corresponding eight-membered ring GBC mechanism seems less favorable in our case. At the same time, a model described above (**11**) that could take advantage of a six-membered ring tertiary amine-catalyzed GBC mechanism was unsuccessful in achieving *o*-quinone hydration. While not ruling out the GBC mechanism, our study demonstrates chemical precedent for facilitation of *o*-quinone hydration by a trihydridynyl-Cu^{II}OH species. Independent of the issue of TPQ biogenesis, to our knowledge, this facilitated hydration is the first demonstration of formal conjugate addition of H₂O (as opposed to H₂O₂) to an *o*-quinone.

Experimental Section

General Procedures. NMR spectra were obtained on Varian Gemini 200 and 300 instruments (¹³C NMR at 50 and 75 MHz, respectively), with chemical shifts being referenced to the TMS or solvent peak. High-resolution mass spectrometry (HRMS; FAB) spectra were obtained on a Kratos MS-25A instrument. UV-vis spectra were obtained using a Perkin-Elmer Lambda 20 spectrophotometer equipped with a temperature-controlled multiple-cell compartment. 4-*tert*-Butyl-1,2-benzoquinone (**5**)¹³ and 2-hydroxy-5-*tert*-butyl-1,4-benzoquinone (**6**)²¹ were prepared as shown previously. Bis(2-pyridylethyl)amine was prepared according to a literature procedure.²² The NH₃/MeOH used for chromatography was prepared by saturation of dry MeOH with dry NH₃ followed by a 2-fold dilution with dry MeOH. The HCl/EtOH solution used for deprotecting Boc-protected ligands was made by saturation of absolute EtOH with dry HCl, followed by a 10-fold dilution with absolute EtOH. The CO₂-free Nanopure water used for titration and kinetic studies was purified by a Milli-Q water purification system from Millipore and was boiled before use.

Synthesis of Models. A. *N,N*-Bis(2-pyridylmethyl)ethanediamine (BPEN) Trihydrochloride.²³ A solution of Boc₂O (21.8 g, 100 mmol) in 90 mL of THF was added over 30 min to a well-stirred solution of ethylenediamine (30 mL) in 80 mL of THF and 10 mL of water at 0 °C. The mixture was then stirred at room temperature for 2 days. The solvent was removed under reduced pressure, and the residue was partitioned between 200 mL of EtOAc and 100 mL of brine. The

organic layer was separated, washed with brine (2 × 50 mL), dried over Na₂SO₄, and evaporated to give *N*-(2-aminoethyl)carbamic acid *tert*-butyl ester as a colorless oil (15.2 g, 95% yield based on starting Boc₂O).

A mixture of the latter ester (2.4 g, 15 mmol), 2-picoyl chloride hydrochloride (5.0 g, 30.5 mmol), and NaOH (2.4 g, 60 mmol) in 100 mL of THF and 100 mL of water was stirred at 50 °C for 5 days. The organic layer was separated, and the aqueous layer was extracted with CH₂Cl₂ (100 mL). To the combined organic layer were added Boc₂O (2.0 g, 9.2 mmol) and Et₃N (20 mL), and the mixture was stirred at room temperature overnight. The solvent was removed, and the residue was separated by silica gel flash chromatography using hexanes–EtOAc–MeOH/NH₃ (7:3:0.5) as eluent to give *N*-(2-(bis(2-pyridylmethyl)amino)ethyl)carbamic acid *tert*-butyl ester (4.67 g, 13.6 mmol, 91%) as a light brown viscous oil: ¹H NMR (CDCl₃) δ 1.40 (s, 9H), 2.66 (t, 2H, *J* = 5.8 Hz), 3.19 (q, 2H, *J* = 5.8 Hz), 3.82 (s, 4H), 5.87 (br, 1H, NH), 7.11 (t, 2H, *J* = 6.1 Hz), 7.38 (d, 2H, *J* = 7.7 Hz), 7.60 (dt, 2H, *J* = 1.0, 7.6 Hz), 8.85 (ddd, 2H, *J* = 0.8, 1.6, 4.8 Hz); ¹³C NMR (APT, CDCl₃) δ 28.5 (–), 38.5 (+), 53.6 (+), 60.2 (+), 78.8 (+), 122.1 (–), 123.1 (–), 136.5 (–), 149.1 (–), 156.2 (+), 159.3 (+). The small amount of Boc-protected secondary amine (side product) was not characterized. The Boc protection was used to facilitate separation of the otherwise coeluting secondary and tertiary amines.

A solution of *N*-(2-(bis(2-pyridylmethyl)amino)ethyl)carbamic acid *tert*-butyl ester (3.0 g, 8.8 mmol) in 40 mL of HCl/EtOH was stirred at room temperature overnight. The mixture was evaporated to dryness to give BPEN·3HCl (3.0 g, 8.5 mmol, 97%) as a light brown amorphous solid: ¹H NMR (CD₃OD) δ 3.02 (t, 2H, *J* = 5.8 Hz), 3.35 (t, 2H, *J* = 5.8 Hz), 4.35 (s, 4H), 8.09 (ddd, 2H, *J* = 1.1, 5.9, 7.5 Hz), 8.26 (d, 2H, *J* = 7.9 Hz), 8.65 (dt, 2H, *J* = 1.6, 7.9 Hz), 8.90 (dd, 2H, *J* = 1.0, 5.9 Hz); ¹³C NMR (APT, CD₃OD) δ 37.9 (+), 53.4 (+), 56.8 (+), 127.9 (–), 129.1 (–), 143.2 (–), 148.7 (–), 153.4 (+).

B. 4-(2-(Bis(2-pyridylmethyl)amino)ethylaminomethyl)-1,2-benzenediol Trihydrochloride (1·3HCl). To a solution of BPEN·3HCl (1.16 g, 3.3 mmol) in 50 mL of methanol was added solid NaOH (0.4 g, 10 mmol). The mixture was stirred at 50 °C until all the NaOH was dissolved. The resulting suspension was evaporated to dryness, and the residue was extracted with 50 mL of 2-propanol. Solid NaCl was filtered off, and the filtrate was evaporated to dryness. The dry free base of BPEN was mixed with 1 mL of HOAc and 3,4-dihydroxybenzaldehyde (0.51 g, 3.6 mmol) in 50 mL of 2-propanol. The mixture was stirred at 50 °C for 10 min, and then evaporated to dryness. The resulting Schiff base was further dried by two rounds of dissolving in 2-propanol (50 mL each) and subsequent evaporation. The dry Schiff base was dissolved in 2 mL of HOAc and 50 mL of MeOH, to which was added solid NaBH₄ (0.5 g, 13.3 mmol) in small portions with stirring. The mixture was further stirred at room temperature for 30 min, and then 5 mL of 12 N aqueous HCl was added. The mixture was evaporated to dryness, leaving a white residue to which were added 100 mL of CH₂Cl₂, Boc₂O (2.6 g, 12 mmol), and 20 mL of Et₃N. The resulting mixture was stirred at room temperature overnight, and the solvent was removed, leaving a residue that was purified by silica gel flash chromatography using hexanes–EtOAc–MeOH/NH₃ (7:3:0.5, v/v) as eluent to afford tri-Boc-protected ligand **1** as a mixture of two amide rotamers (1.75 g, 2.6 mmol, 79%): colorless oil; ¹H NMR (CDCl₃) δ 1.34 and 1.41 (2s, 9H total), 1.526 (s, 9H), 1.530 (s, 9H), 2.68 (m, 2H), 3.25 and 3.36 (2t, 2H total), 3.81 (s, 4H), 4.26 and 4.38 (2s, 2H total), 6.9–7.2 (5H), 7.48 (m, 2H), 7.65 (m, 2H), 8.51 (m, 2H).

The above tri-Boc-protected ligand (1.75 g) was deprotected by dissolution in HCl/EtOH and heating at 50 °C for 5 min, followed by evaporation of the solution to give **1**·3HCl (1.23 g, 2.6 mmol, 100%) as a white amorphous solid: ¹H NMR (CD₃OD) δ 3.08 (t, 2H, *J* = 7.8 Hz), 3.35 (t, 2H, *J* = 7.8 Hz), 4.14 (s, 2H), 4.34 (s, 4H), 6.72 (d, 1H, *J* = 8.1 Hz), 6.87 (dd, 1H, *J* = 2.2, 8.1 Hz), 7.01 (d, 1H, *J* = 2.2 Hz), 8.05 (t, 2H, *J* = 6.4 Hz), 8.21 (d, 2H, *J* = 7.9 Hz), 8.65 (dt, 2H, *J* =

(20) Prabhakar, R.; Siegbahn, P. E. M. *J. Am. Chem. Soc.* **2004**, *126*, 3996–4006.

(21) Lee, Y.; Sayre, L. M. *J. Am. Chem. Soc.* **1995**, *117*, 11823–11828.

(22) Brady, L. E.; Freifelder, M.; Stone, G. R. *J. Org. Chem.* **1961**, *26*, 4757–4758.

1.4, 7.9 Hz), 8.90 (dd, 2H, $J = 1.1, 5.8$ Hz); ^{13}C NMR (APT, CD_3OD) δ 45.1 (+), 52.5 (+), 57.0 (+), 116.7 (–), 118.7 (–), 123.1 (+), 123.6 (–), 127.9 (–), 129.0 (–), 143.2 (–), 146.7 (+), 147.8 (+), 148.7 (–), 153.3 (+); HRMS (FAB) m/z calcd for $\text{C}_{21}\text{H}_{25}\text{N}_4\text{O}_2$ (MH^+) 365.1978, found 365.1967 (rel intens 100).

C. *N'*-(3,4-Dimethoxybenzyl)-*N,N*-bis(2-pyridylmethyl)ethane-diamine Trihydrochloride (2·3HCl). The dry free base BPEN prepared from 1.16 g of BPEN·3HCl as for **1** above was dissolved in 50 mL of 2-propanol, and 3,4-dimethoxybenzaldehyde (0.61 g, 3.6 mmol) was added. The mixture was stirred at 60 °C for 10 min before evaporation to dryness. The residual water was removed azeotropically using benzene (2 × 50 mL). The resulting dry Schiff base was dissolved in 50 mL of absolute EtOH, and solid NaBH_4 (0.5 g, 13.3 mmol) was then added in small portions with stirring. After being further stirred for 30 min, the mixture was acidified with 12 N aqueous HCl to pH 1 and then evaporated to dryness. The residue was suspended in 100 mL of CH_2Cl_2 , and Boc_2O (1.1 g, 5 mmol) and Et_3N (20 mL) were added. The mixture was stirred for 30 min and evaporated to dryness. The residue was purified by silica gel flash chromatography using hexanes–EtOAc– NH_3/MeOH (6:1:0.7, v/v) as eluent to give the Boc-protected form of amine **2**. The latter compound was dissolved in 50 mL of HCl/EtOH, and the mixture was heated at 50 °C for 10 min. Evaporation to dryness gave 2·3HCl (1.37 g, 2.72 mmol, 82%) as a pale solid: mp 209–211 °C dec; ^1H NMR (CD_3OD) δ 3.09 (t, 2H, $J = 4.6$ Hz), 3.38 (t, 2H, $J = 4.6$ Hz), 3.82 (s, 3H), 3.88 (s, 3H), 4.23 (s, 2H), 4.33 (s, 4H), 6.95 (d, 1H, $J = 8.0$ Hz), 7.10 (dd, 1H, $J = 0.75, 8.0$ Hz), 7.32 (d, 1H, $J = 0.75$ Hz), 8.04 (t, 2H, $J = 6.6$ Hz), 8.19 (d, 2H, $J = 8.0$ Hz), 8.59 (t, 2H, $J = 7.7$ Hz), 8.86 (d, 2H, $J = 5.7$ Hz); ^{13}C NMR (APT, CD_3OD) δ 45.4 (+), 52.6 (+), 52.7 (+), 56.5 (–), 56.8 (–), 57.0 (+), 112.8 (–), 115.2 (–), 124.5 (+), 124.6 (–), 127.9 (–), 129.0 (–), 143.2 (–), 148.5 (–), 150.7 (+), 151.5 (+), 153.5 (+); HRMS (FAB) m/z calcd for $\text{C}_{23}\text{H}_{29}\text{N}_4\text{O}_2$ (MH^+) 393.2291, found 393.2294 (rel intens 100).

D. 5-(2-(Bis(2-pyridylmethyl)amino)ethylaminomethyl)-1,2,4-benzotriol Trihydrochloride (3·3HCl). A solution of BPEN·3HCl (352 mg, 1 mmol) in 20 mL of MeOH was treated with solid NaOH (120 mg, 3 mmol) as for **1**. The dry free base BPEN was dissolved in 20 mL of 2-propanol, and 1 mL of HOAc and 2,4,5-trihydroxybenzaldehyde (169 mg, 1.1 mmol) were added. The mixture was stirred at 50 °C for 10 min and evaporated to dryness. Trace water was removed by evaporation of the residue twice with 2-propanol (2 × 10 mL). The final Schiff base was dissolved in 2 mL of HOAc and 20 mL of MeOH, and solid NaBH_4 (250 mg, 6.6 mmol) was then added in small portions with stirring. After the mixture was further stirred for 30 min, 2 mL of 12 N aqueous HCl was added, and the mixture was evaporated to dryness. The residue was suspended in 50 mL of CH_2Cl_2 , and then Boc_2O (1.31 g, 6 mmol) was added. The mixture was purged with argon for 5 min and sealed with a septum. Degassed Et_3N (5 mL) was introduced by syringe, and the mixture was stirred at room temperature overnight. Evaporation of the suspension, followed by silica gel flash chromatography of the residue using hexanes–EtOAc– NH_3/MeOH (7:3:0.5, v/v) as eluent, afforded the tetra-Boc-protected form of triol **3**. The latter compound was dissolved in 20 mL of HCl/EtOH, and the mixture was heated at 50 °C for 5 min. Evaporation of the solution to dryness gave 3·3HCl (318 mg, 0.65 mmol, 65%) as a light brown amorphous solid: ^1H NMR (CD_3OD) δ 3.05 (t, 2H, $J = 6.1$ Hz), 3.30 (t, 2H, $J = 6.1$ Hz), 4.12 (s, 2H), 4.32 (s, 4H), 6.38 (s, 1H), 6.81 (s, 1H), 8.04 (ddd, 2H, $J = 1.2, 5.9, 7.2$ Hz), 8.17 (d, 2H, $J = 7.7$ Hz), 8.59 (dt, 2H, $J = 1.6, 7.9$ Hz), 8.86 (ddd, 2H, $J = 0.5, 1.5, 5.9$ Hz); ^{13}C NMR (APT, CD_3OD) δ 44.6 (+), 47.6 (+), 52.3 (+), 57.0 (+), 104.4 (–), 108.2 (+), 119.4 (–), 127.9 (–), 128.9 (–), 139.4 (+), 143.1 (–), 148.6 (–), 148.9 (+), 151.0 (+), 153.4 (+); HRMS (FAB) m/z calcd for $\text{C}_{21}\text{H}_{25}\text{N}_4\text{O}_3$ (MH^+) 381.1927, found 381.1920 (rel intens 100).

A preliminary potentiometric pH titration (see below) showed that the isolated **2** from HCl solution was the tri- rather than tetrahydro-

chloride form. Similar observations have been reported in cases of other dipicolylamine-type ligands,²⁴ including BPEN.²³ It is thus assumed that the isolated models **1** and **3** are also in their trihydrochloride forms.

Coordination Chemistry of Ligand 3 with M(II). A. UV–Vis Titration. A 0.0500 M standard solution of free base ligand **2** in 1:1 (v/v) aqueous MeOH was prepared by dissolving 25.1 mg of 2·3HCl in 1 mL of 0.150 M NaOH in 1:1 aqueous MeOH. A 3 mL quartz cuvette was filled with 1.00 mM CuSO_4 solution in 50% aqueous MeOH (3.00 mL), and the UV–vis spectrum was recorded at 25 °C. Small aliquots (6.0 μL each) of a standard solution of **2** were then added to the cuvette, and the solution was well mixed before the UV–vis spectrum was recorded after each addition. The results are shown in Figure S1.

B. Potentiometric pH Titration. To an argon-protected solution of ligand 2·3HCl (5.00 mM) and HNO_3 (5.00 mM) in 5.00 mL of 0.15 M aqueous KNO_3 in the absence or presence of a metal ion (5.00 mM) were added small aliquots (10.0 μL each) of standard 0.250 M aqueous NaOH with stirring at 25 °C. The titration was monitored by an Accumet model 910 pH meter equipped with a Fisher combination glass electrode. The meter was calibrated to ± 0.01 using commercial standard buffers before each run. Typical titration $a(\text{OH})$ –pH curves are shown in Figure 1A, where $a(\text{OH})$ represents the number of equivalents of added NaOH with respect to the total number of equivalents of ligand or 1:1 ligand/metal complex in solution. To calculate the various equilibrium constants, the collected data were analyzed according to the program BEST,¹⁴ using a $\text{p}K_w$ value of 13.73²⁵ and three metal–ligand species, MHL, ML, and MH_{-1}L , which represent a metal complex with a monoprotonated tridentate ligand, a metal complex with a free base tetradentate ligand, and the metal-bound water-deprotonated form of complex ML, respectively. Using the three species above, the $\sigma(\text{pH})$ fit values defined in the program were less than 0.03 in all cases, but omission of any species from the calculation resulted in high σ values. The speciation diagrams for these titrations were generated using the program SPE,¹⁴ as exemplified by that for the 2–Cu(II) system (Figure 1B). To confirm the involvement of MHL, ML, and MH_{-1}L , the same pH titration of the 2–Cu(II) system was repeated, with 3 mL aliquots being frequently removed for UV–vis measurement and then transferred back to continue the titration. The results are shown in Figure S2.

Oxidation of 4-*tert*-Butylcatechol (4) with Periodate in pH 7.50 MOPSO Buffer. To a 3 mL quartz cuvette were added 30.0 μL of 0.010 M catechol **4** or hydroxyquinone **6** in dioxane, 3.00 mL of 0.05 M pH 7.5 MOPSO buffer, and 6.0 μL of 0.1 M aqueous NaIO_4 . The solution was quickly mixed and subjected to UV–vis monitoring at 25 °C (Figure S3). The difference spectra were generated using Origin software (version 7.5) by subtracting the first spectrum from all other spectra obtained thereafter.

In another experiment, a mixture of 30.0 μL of 0.010 M **4** or **6** in dioxane and 3.0 μL of 0.100 M aqueous CuSO_4 was diluted to 3.00 mL with 0.05 M pH 7.5 MOPSO buffer. The reaction was initiated by addition of 6.0 μL of 0.1 M aqueous NaIO_4 and then subjected to UV–vis monitoring (Figure S4 in the Supporting Information).

In the third experiment, **4** and **6** (1×10^{-4} M) were both incubated with a 1:1 complex (1×10^{-4} M) of Cu(II) with bis(2-pyridylethyl)amine and NaIO_4 (2×10^{-4} M) under the same conditions. UV–vis monitoring afforded spectra as shown in Figure S5 in the Supporting Information.

Behavior of Catechol Ligand Model 1. A. Cu(II)-Mediated Quinone Hydration in pH 7.5 MOPSO Buffer and Product Characterization by HPLC. A mixture of 20.0 μL of 10.0 mM

(23) BPEN·3HCl has been synthesized by a different route: Chiu, Y.-H.; Canary, J. W. *Inorg. Chem.* **2003**, *42*, 5107–5116.

(24) See, for example: Sugimoto, H.; Miyake, H.; Tsukube, H. *J. Chem. Soc., Dalton Trans.* **2002**, 4535–4540. Hartshorn, R. M.; Telfer, S. G. *J. Chem. Soc., Dalton Trans.* **2000**, 2801–2808.

(25) Miranda, C.; Escarti, F.; Lamarque, L.; Yunta, M. J. R.; Navarro, P.; Garcia-Espana, E.; Jimeno, M. L. *J. Am. Chem. Soc.* **2004**, *126*, 823–833.

aqueous **1**·3HCl and 2.0 μL of 0.100 M aqueous CuSO_4 was diluted with 0.05 M pH 7.5 MOPSO buffer to 1.00 mL, and then 4 μL of 0.1 M aqueous NaIO_4 was added with stirring at 25 $^\circ\text{C}$. The solution immediately turned red, indicative of hydroxyquinone **7**-Cu(II) arising from oxidation of the initial quinone hydration product **3**-Cu(II). After being further stirred for 1 min, the mixture was acidified with 12 N aqueous HCl. Solid NaBH_4 (10 mg) was added in small portions with maintenance of pH 1–2, and then 10 μL of 0.1 M aqueous diethylenetriaminepentaacetic acid was added. After being further stirred for 2 min, the solution was filtered and subjected to HPLC analysis using an Agilent SB-C18 9.4×250 mm column and aqueous CH_3CN containing 0.02% CF_3COOH as mobile phase, with the composition of CH_3CN increasing from 0 to 35% over 30 min. The same procedure was repeated with authentic triol **3**·3HCl, and the results are shown in Figure S6. Authentic triol **3** was found to survive this oxidation–reduction cycle without significant change as determined by HPLC and UV–vis (not shown).

B. UV–Vis Monitoring of M(II)-Dependent Quinone Hydration in pH 7.5 MOPSO Buffer. To a 3 mL quartz cuvette were added 3.0 μL of 0.100 M aqueous CuSO_4 and 30.0 μL of 0.0100 M aqueous **1**·3HCl or **3**·3HCl, and the mixture was diluted to 3.00 mL using 0.05 M pH 7.5 MOPSO buffer. After further addition of 6.0 μL of 0.1 M aqueous NaIO_4 , the solution was quickly mixed and subjected to UV–vis scanning at 25 $^\circ\text{C}$ (Figure 2A). Similar results were obtained using $\text{Zn}(\text{NO}_3)_2$ and NiSO_4 (not shown). The yields of **7**-M(II) were determined by UV–vis against authentic **7**-M(II) according to the 550 nm absorbance in all cases to avoid interference of side products from decomposition of *o*-quinone that absorb at 500 nm (see below and Figure S7).

C. Decomposition of *o*-Quinone **8 in pH 7.5 MOPSO Buffer and Interaction of the Decomposition Product with M(II).** To a 3 mL quartz cuvette were added 15.0 μL of 0.0100 M aqueous **1**·3HCl or **3**·3HCl, 3.00 mL of 0.05 M pH 7.5 MOPSO buffer, and then 3.0 μL of 0.1 M aqueous NaIO_4 . The solution was quickly mixed and subjected to UV–vis scanning at 25 $^\circ\text{C}$ (Figure 2B). In another three runs of the same reaction with **1**·3HCl, the final oxidation mixtures were mixed with 1.5 μL of 0.100 M aqueous CuSO_4 , $\text{Zn}(\text{NO}_3)_2$, and NiSO_4 , respectively, and the UV–vis spectra were recorded immediately (Figures 2B and S7).

D. Cu(II)-Mediated Quinone Hydration in pH 7.5 Phosphate Buffer. Using a procedure similar to that above, oxidations of **1**·3HCl or **3**·3HCl (1×10^{-4} M) were conducted in 0.05 M pH 7.5 phosphate buffer at 25 $^\circ\text{C}$ in the presence of CuSO_4 (1×10^{-4} M). Upon initiation of the reactions with periodate (2×10^{-4} M), the UV–vis spectra were immediately recorded. In another run, the same oxidation of **1**·3HCl was conducted without CuSO_4 . After the UV–vis spectrum was recorded, 1 equiv of CuSO_4 was added, and the UV–vis spectrum was recorded again. The results are summarized in Figure S8.

E. Time-Dependent Formation of **7-Cu(II) in pH 4.00 Acetate Buffer.** To a 3 mL quartz cuvette were added 3.0 μL of 0.100 M aqueous CuSO_4 and 30.0 μL of 0.0100 M aqueous **1**·3HCl. The mixture was diluted to 3.00 mL using 0.05 M pH 4.00 acetate buffer. After further addition of 6.0 μL of 0.1 M aqueous NaIO_4 , the solution was quickly mixed and subjected to UV–vis scanning at 25 $^\circ\text{C}$. The result is shown in Figure 3.

F. Kinetic Studies of Quinone Hydration as a Function of pH Using Mixed Universal Buffers. Mixed buffer solutions composed of 0.1 M acetate, 0.05 M 4-morpholineethanesulfonic acid (MES), and 0.05 M 4-(2-hydroxyethyl)-1-piperazineethanesulfonic acid (HEPES) from pH 5.00 through pH 8.50 in 0.25 pH unit increments were prepared and cooled to 10 $^\circ\text{C}$. To a 3 mL quartz cuvette at 10 $^\circ\text{C}$ were added 3.0 μL of 0.100 M aqueous CuSO_4 and 30.0 μL of 10.0 mM aqueous **1**·3HCl. The mixture was diluted to 3.00 mL using the cooled mixed buffers. After further addition of 6 μL of 0.1 M aqueous NaIO_4 , the solution was quickly mixed, and A_{550} was recorded over time at 10 $^\circ\text{C}$ (see Figure S9 in the Supporting Information for an example). The data were treated using Origin software (version 7.5) to yield the observed first-order rate constants k_{obsd} (correlation coefficients r were always > 0.999), which were plotted against pH to give the pH–rate profiles as shown in Figure 3 (inset). A nonlinear least-squares fit to the pH–rate profile for the **1**-Cu(II) system over the pH range 5.00–8.00 was achieved (Origin 7.5) according to the equation $k_{\text{obsd}} = kK_{\text{app}}/(K_{\text{app}} + \alpha_{\text{H}^+})$, where K_{app} represents the apparent ionization constant of the Cu(II)-bound water, k represents the real rate constant of the dissociated complex species **8**- M^- , and α_{H^+} represents the proton activity of the reaction system. The kinetic data for Zn(II) and Ni(II) were obtained following the same procedure. The formation of hydroxyquinone **7** was observed only at pH > 6.5 for Zn(II) and pH > 7.25 for Ni(II). The results are also shown in Figure 3 (inset).

Acknowledgment. We thank the National Institutes of Health for support of this work through Grant GM 48812.

Supporting Information Available: UV–vis titration of Cu(II) with ligand **2**, UV–vis monitoring of periodate oxidations of catechol **4**, HPLC diagrams and the diode array spectra for characterization of hydroxyquinone **7**, UV–vis spectra showing decomposition of *o*-quinone **8** in the absence of M(II) and interaction of the resulting solution with Cu(II), Zn(II), and Ni(II), and typical time driven UV–vis monitoring of M(II)-dependent quinone hydration with first-order kinetics plots (PDF). This material is available free of charge via the Internet at <http://pubs.acs.org>.

JA0455603